Crystal Structure of FMN-Dependent Nitroreductase from *Escherichia coli* B: A Prodrug-Activating Enzyme[†,‡]

Gary N. Parkinson, Jane V. Skelly, and Stephen Neidle*

CRC Biomolecular Structure Unit, Chester Beatty Laboratories, The Institute of Cancer Research, London SW3 6JB, United Kingdom

Received April 6, 2000

The FMN-dependent flavoprotein nitroreductase from *Escherichia coli* B (NTR) is used in cancer chemotherapy to activate a range of prodrugs. The crystal structure of this enzyme has been determined, using molecular replacement methods and refined at 2.06 Å resolution. The recombinant 24-kDa enzyme was crystallized in the tetragonal space group $P4_12_12$, with unit cell dimensions of $a = b = 57.74$ Å and $c = 275.51$ Å and two molecules in the asymmetric unit. The structure has a final R factor of 20.3% ($R_{free} = 26.7\%$), for all data between the resolution ranges of 10−2.06 Å, and includes 4453 protein atoms, 230 water molecules, and 2 flavin mononucleotide (FMN) molecules. The functional unit is a homodimer, which forms the asymmetric unit in the crystal structure. The tertiary structures of these two monomers and their subunit interactions are nearly identical. The molecular replacement search model, the crystal structure of the major NAD(P)H:FMN oxidoreductase of *Vibrio fisheri* (FRase 1), was selected on the basis of its high sequence identity to that of NTR. The final superposition of these two enzymes revealed a very similar overall fold, with variation in the structures focused around surface loops and helices near the FMN cofactor. Helix G is implicated in substrate specificity and is better resolved in the present NTR structure than in the previously reported FRase 1 structure. The FMN binding pocket is also well-resolved, showing the presence of two channels leading into the active site. The amino acid side chains and main chain atoms interacting with the FMN are well-ordered. The structure of the substrate binding pocket has been used to examine substrate specificity and enzyme kinetics for prodrugs used in antibody-directed enzyme prodrug therapy (ADEPT) and gene-directed enzyme prodrug therapy (GDEPT).

Introduction

The FMN-dependent nitroreductase enzyme from *Escherichia coli* B (NTR) reduces a range of nitro-containing substrates. It is capable of reducing nitrofurazone, a feature in common with the "classical nitroreductase" of *Salmonella typhimurium*[1] and *Enterobacter cloacae*.[2] In addition, the enzyme can reduce quinones, such as menadione, and be inhibited by dicoumarol, a property shared by the mammalian enzyme DT-diaphorase (NAD(P)H oxidoreductase).[3] The ability of this enzyme to reduce nitro groups to the corresponding hydroxylamines has led to its use in studies to activate prodrugs containing a nitro group into antitumor agents. These hydroxylamines can be further activated, resulting in the formation of cytotoxic DNA cross-linking agents. The ability of NTR to reduce a range of dinitrophenylcarboxamides has highlighted its potential usefulness in gene therapy for the tumor-selective activation of cytotoxic alkylating drugs and has since been used in several prodrug approaches such as ADEPT (antibody-directed enzyme prodrug therapy), GDEPT (gene-directed), and VDEPT (viral-directed), notably with the aziridinyl prodrug CB1954 (5-(aziridin-1-yl)-2,4-dinitrobenzamide; Figure 1, **1**).[4] Enhanced reductive activation to a cytotoxic DNA cross-linking agent has also been achieved with the use of mustard prodrugs such as SN23862 (Figure 1, **2**).

NTR is one member of a structurally homologous family,[5] containing to date four flavoproteins whose crystal structures have been solved. Within this family the position of the FMN cofactor is related to the tertiary structure and is highly conserved, with the *re* face solvent-accessible. The enzymes also exhibit low substrate specificity. The family can be divided into two subgroups: nitroreductases, of which NTR is a member, and flavin reductases, of which FRase 1 is a member. The nitroreductase group can be further divided into oxygen-sensitive and oxygen-insensitive members.

The present crystal structure determination shows that NTR is a tightly associated homodimer with the FMN bound within a crevice formed by the dimer interface. It is known that the enzyme uses FMN as an enzyme-bound cofactor to mediate the two-electron transfer. The electron transfer from NAD(P)H proceeds as the first step in the ping-pong Bi−Bi reaction pathway. The structure shows two channels that could

[†] This work was supported by the Cancer Research Campaign (Program Grant SP1384 to S. Neidle).

[‡] Abbreviations: FMN, flavin mononucleotide; FAD, flavin adenine dinucleotide; NTR, nitroreductase enzyme; ADEPT, antibody-directed enzyme prodrug therapy; GDEPT, gene-directed enzyme prodrug therapy; VDEPT, viral-directed enzyme prodrug therapy; PEG, poly(ethylene glycol); FRase 1, NAD:FMN oxidoreductase enzyme; NOX, NADH oxidase enzyme; FRP, flavin reductase P enzyme.

* To whom correspondence should be addressed: Prof. S. Neidle, CRC Biomolecular Structure Unit, Chester Beatty Laboratories, The Institute of Cancer Research, 237 Fulham Rd., London SW3 6JB, U.K. Tel: 0044 20 7970 6043. Fax: 0044 20 7352 8039. E-mail: s.neidle@icr.ac.uk.

10.1021/jm000159m CCC: $19.00
Published on Web 09/09/2000

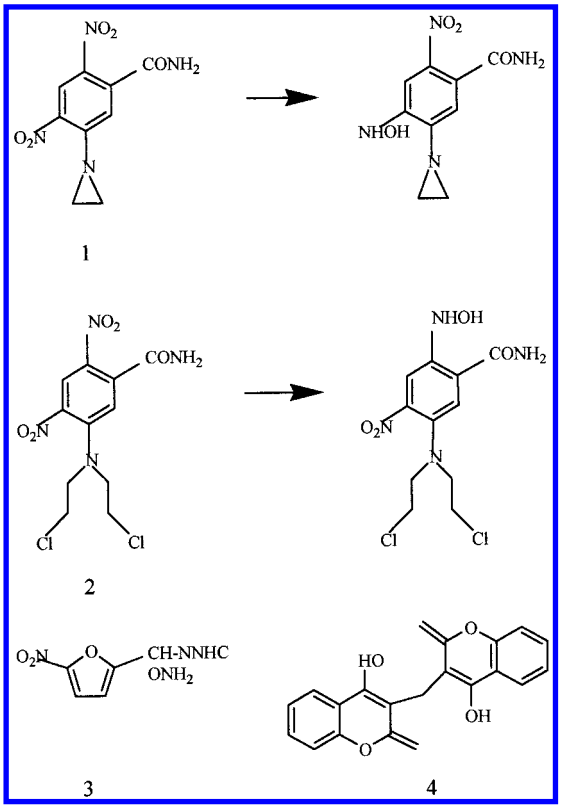

Figure 1. Major substrates and an inhibitor for NTR. (**1**) The prodrug CB1954 is shown together with one of the two possible activated forms, the 4-hydroxylamine. (**2**) The prodrug SN23862, a possible candidate for GDEPT containing a difunctional alkylating agent, shown with the 2-hydroxylamine product. It is reduced by NTR at the 2-position; however it is not reduced by rat DT diaphorase. (**3**) Nitrofurazone. (**4**) Dicoumarol, which acts as a competitive inhibitor of CB1954 with both NTR and DT diaphorase.

facilitate access of substrates to the FMN. One is open and does not require any modification of the structure to allow access of NAD(P)H or the prodrug CB1954, while the second is closed by Phe124 from helix G projecting into the binding pocket. On the basis of the previous study on the homologous protein FRase 1,[6] modifications of Phe123 or Phe124 in the NTR protein would result in increased flavin reductase activity. These two residues form part of the cofactor and substrate binding pocket and will be discussed below. The focus of this article is to analyze the possible mechanism of activation and further to provide a basis for the rational design of more effective NTR prodrugs.

Results and Discussion

Overall Structure. The structure consists of a physiological homodimer of 48 kDa, with the two molecules of FMN located within crevices formed at the dimer interface (Figure 3). Each monomer consists of 217 amino acids, forming a five-stranded β-sheet folded in an $\alpha + \beta$ motif. The β-sheets form four antiparallel strands with a fifth strand from the C-terminus of the second monomer interacting with FMN, as shown in Figure 3. The monomer consist of three main domains: a core domain including residues 2−89 and residues 135−180, a flexible region containing residues 90−134, and a region tightly associated with the second monomer, residues 181−206. The rms deviation between all Cα atoms of the two monomers A and B is 0.90 Å. The largest rms differences observed are for surface loops and for α-helix G, which is contained within the flexible region that shows higher than average *B*-factors. Residues 127−133, comprising a surface loop at the end of helix G, show the poorest electron density of the entire structure. This disorder is seen in both monomers A and B, although to a greater extent in the latter. Residues involved in FMN binding are highly ordered; however, the flexible and more poorly resolved residues from helix G form part of the opening to the cofactor and substrate binding pocket.

There are only small differences between NTR and the search model FRase 1. The rms deviation between Cα atoms of one monomer NTR and a corresponding monomer of FRase 1 is 1.4 Å, highlighting the similarity of the two proteins. The two structures also share similar temperature factor distributions throughout the structure except in the region of helix G, where we observe good electron density along the length of the helix. The largest rms deviations between both structures, for both Cα and side chain atoms, are within this region. On the basis of the sequence alignment, there is a significant difference in amino acid sequence identity between the two proteins within helix G, which may reflect substrate specificity.

NTR Compared to Other Structurally Homologous Flavoproteins. All four enzymes NTR, FRase 1,[6] FRP,[7] and NOX[8] are members of a novel flavoprotein family. They exhibit little sequence or structural homology to other flavoproteins. The core regions of all four enzymes are structurally equivalent, suggesting a common ancestral flavoprotein. In all cases FMN is tightly bound in the active site, with many conserved hydrogen bonds and hydrophobic interactions (Figures 4 and 5). The closest structural homology exists between NTR and FRase 1. When comparing NTR to FRase 1, the most conserved regions in the sequence are those residues involved in FMN binding, particularly residues 10−25, 40−55, and 193−207. The greatest variation in sequence is between residues 116−124. This region overlaps helix G of NTR and may convey substrate specificity. Both NTR and FRase 1 can use either NADH or NADPH as electron donors, while FRP exclusively uses NADPH. The similarity of NTR to NOX is seen in the overall topology of their secondary and tertiary structures. This similarity is extensive, again except for helix G of NTR, which matches a small flexible and unstructured domain in the NOX structure. Of the four structures so far solved, only NOX can accommodate either FMN or flavin adenine dinucleotide (FAD) as a cofactor, requiring only very minor shifts in amino acid side chain positions.[6]

FMN Cofactor and Substrate Binding Pocket. The similarity of the two FMN and substrate binding pockets and the relative position of the FMN cofactors within these binding pockets of NTR is highlighted by the small rms deviation between them, 0.5 Å for all main chain atoms within 5 Å of the FMN molecules. Both the FMN cofactors and residues forming the binding pocket are well-ordered, as shown by the $2F_o - F_c$ electron density map contoured at 1.0σ (Figure 4). Each cofactor has a total of 12 hydrogen bonds to the protein and 3 from well-ordered water molecules (Figure

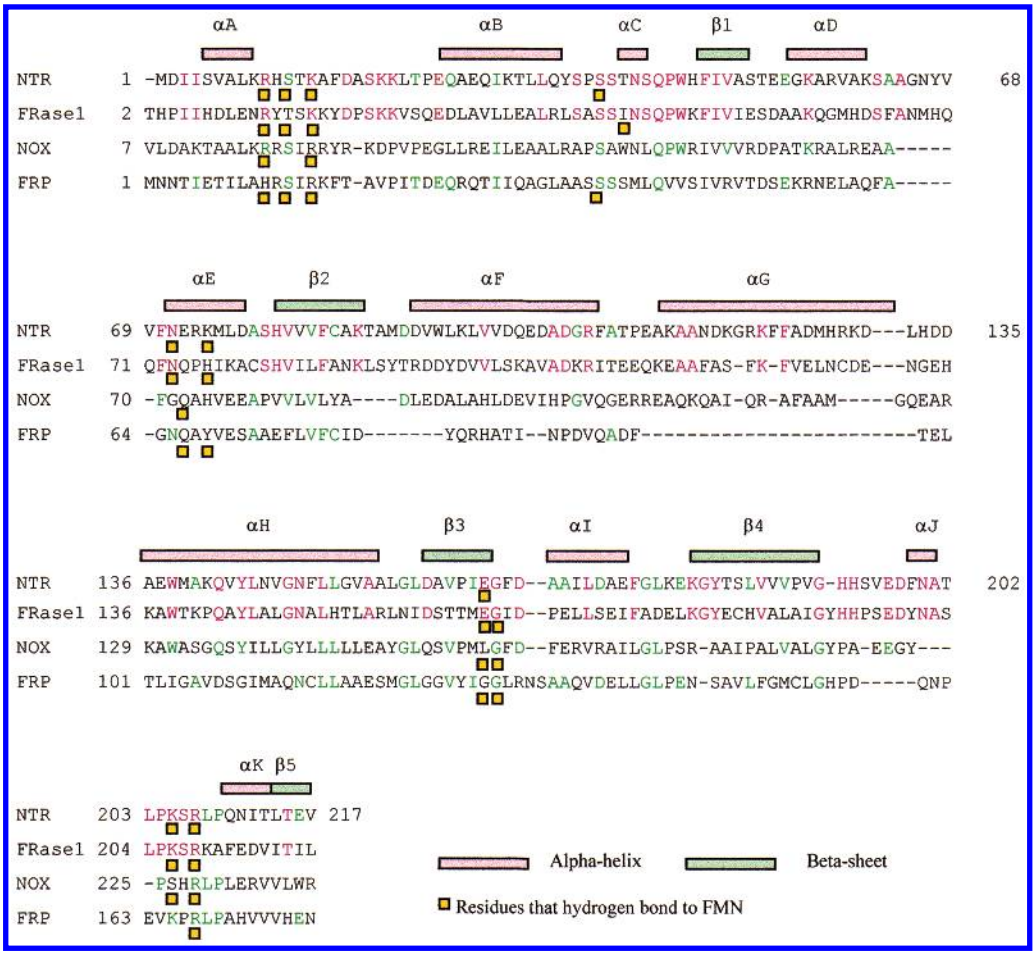

Figure 2. Structure-based sequence alignment of NTR, FRase 1, NOX, and FRP. Secondary structural elements of the NTR are shown as red boxes for α-helical regions and green boxes for *β*-sheets. Regions of protein−FMN interaction are highlighted by yellow boxes. Absolutely conserved amino acid residues between NTR and FRase 1 are shaded in red. Amino acid residues absolutely conserved between NTR, FRP, and NOX are shaded in green. The residue numbers for each protein are shown.

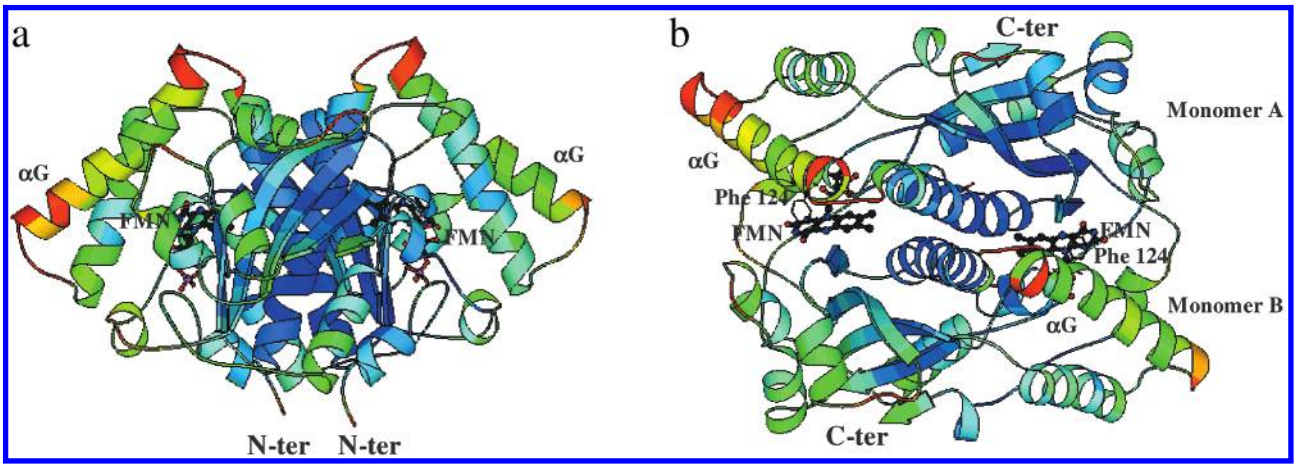

Figure 3. (a) Ribbon diagram of one monomer from the structure of *E. coli* NTR B with attached cofactor FMN, drawn with MOLSCRIPT,[24] colored according to temperature factor size. (b) Structure rotated by 90°. N- and C-terminal regions are labeled, together with residue Phe123 from helix G.

5b). The cofactors are held firmly in place, as evidenced by their high binding affinity. Extraction of the FMN can be accomplished by unfolding the protein on heating to 70 °C.[9]

Within the NTR family of flavoproteins the positioning of the FMN coenzyme in relation to the overall protein conformation is highly conserved. As previously observed in the other structurally homologous proteins, the *re*[10] face is solvent-accessible while the *si* face is buried. Also conserved are residues involved in the binding and hence fixing the orientation of the FMN cofactors. On the basis of the sequence alignment and the structure (Figure 2), it is clear that there are five conserved regions within the protein sequences that are used for FMN binding. First, the C-terminal residues from the second monomer, specifically Arg207 and Lys205; these are placed to interact with the phosphate of FMN from the first monomer. This ensures that the

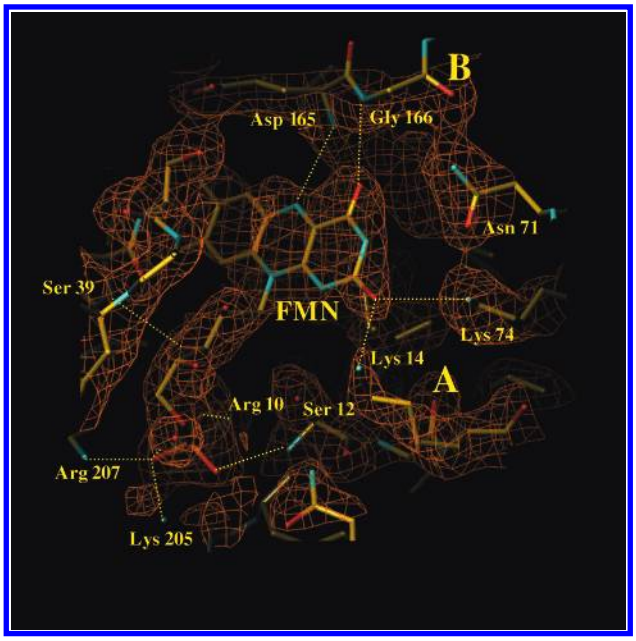

Figure 4. FMN binding pocket associated with monomer A overlaid with a $2F_o - F_c$ electron density map calculated from the final model contoured at 1.0σ. Hydrogen bonds < 3.3 Å ± 1 std are shown by dashed yellow lines. The two potential channels for substrate access to FMN are shown labeled as A and B.

homodimer is in the active conformation. Second, residues Val145 and Tyr144 interact with the benzenoid portion of FMN, by means of hydrophobic interactions. A third set of conserved residues is the amide groups of Glu165 and Gly166, which interact with the N5, O4 face of the isoalloxazine ring system of FMN. These interactions consist of main chain nitrogen atoms hydrogen-bonding to N5 and the carboxyl O4 of FMN. N5 is an important candidate to receive the hydride ion from NADH. The next two regions of interaction are residues 10−13 and 39−41. They are involved in interactions with the ribityl chain. The final conserved region involves residues 72−75, which interact with the pyrimidine O2, N3, O4 face of the FMN. The pyrimidine ring generates a complementary hydrogen-bonding pattern that is comprised of acidic amino acid side chains and waters.

On the basis of structural overlap, it is clear that there are several common protein−FMN interactions found within this family of enzymes, near the pyrimidine ring (Figure 5a). One conserved set consists of two adjacent amino acids interacting with the N5 and O4 of FMN via backbone amides. The first amino acid has an acidic functional group; both the NTR and FRase 1 structures contain a conserved Glu, while the second residue is a conserved Gly. Common to all four structures are donor−acceptor−donor hydrogen-bonding arrangements of the protein side chains, complementing that of the pyrimidine ring of FMN. Both NTR and FRase 1 use a Lys residue to hydrogen-bond to O2 and an Asn residue to hydrogen-bond to N2 and O4 of FMN, while FRP and NOX use the same functionally analogous residues, Arg and Gln.

The substrate pocket containing the bound FMN is V-shaped, narrowing toward FMN itself. Using a water oxygen atom as a probe, the maximum access into the pocket was found to be limited to the third ring of the FMN molecule, which sits at the base of the binding pocket, allowing access to the *re* face by planar substrates. Access to the substrate binding pocket is possible via two openings, labeled A and B (Figure 4). These two openings are separated by a set of residues (70−75) sitting on the surface of the protein. Opening A is lined by hydrophobic residues adjacent to the FMN cofactor, while the interior of the channel is lined with charged residues. Opening A is sufficient to provide access to either NADH or substrates such as CB1954 without conformational change. The shape of the smaller opening (B) is dependent on the conformation of helix G. In our structure this conformation is well-defined; it is notable that this ordering was not observed in any of the previously reported structures not containing a substrate. However, this helix became ordered when an inhibitor was bound, as shown in the FRase 1 structure. This helix may thus be important in defining substrate specificity, particularly as it contains a two-amino acid addition, between residues 119 and 124, when compared to FRase 1. The addition of these two residues results in a change of amino acid sequence alignment for the side chains. Residues at both the N- and C-termini of helix G of NTR are not aligned with FRase 1. However, by moving from the N-terminus to the point of the first amino acid insertion, Gly120, the central region of helix G then is shifted into register. This places Phe124 of helix G in the substrate binding pocket, planar to the FMN isoalloxazine ring system above the central pyrazine ring, as seen in FRase 1. We would then expect the inhibitor dicoumarol, to bind in a similar manor to that observed in the FRase 1 structure. The structure of helix G in NTR after residue 128 matches that of the FRase 1 bound to the inhibitor. Helix G then contains residues that alter the shape of channel (B) and may then define substrate specificity. On the basis of a simple sequence alignment of NTR, Lys122 would be placed incorrectly above FMN, in the place of residue Phe124.

FMN and Substrate Reduction. The reduction of the nitro and quinone compounds requires a two-electron transfer.[11] This proceeds as a ping-pong Bi−Bi reaction. First, the substrate NADH must enter, be oxidized, and leave as NAD+ before the second substrate CB1954 can bind. The hydride transfer should proceed via the *re* face of FMN as the *si* is buried. The dimethyl edge of FMN is also buried and therefore probably not involved in electron transfer. The reduction of FMN by NAD(P)H should result in a small conformational change in the central pyrazine ring, resulting in a butterfly conformation overall for the FMN molecule. Reduction of FMN may then modify the shape of the substrate binding pocket resulting in the structure as described in the present X-ray structure, since we have solved the oxidized form of FMN. Previous studies[12] have shown that both N1 and N5 are candidates for receiving the hydride from NAD(P)H. In this structure, the N1 is available for hydride transfer, while the presence of the N5 hydride is in conflict with the orientation of the main chain amide of Glu165 and thus may not be a suitable site for hydride transfer without conformational change.

Substrate Specificity for the Enzyme Family. We can highlight key features of substrate binding and

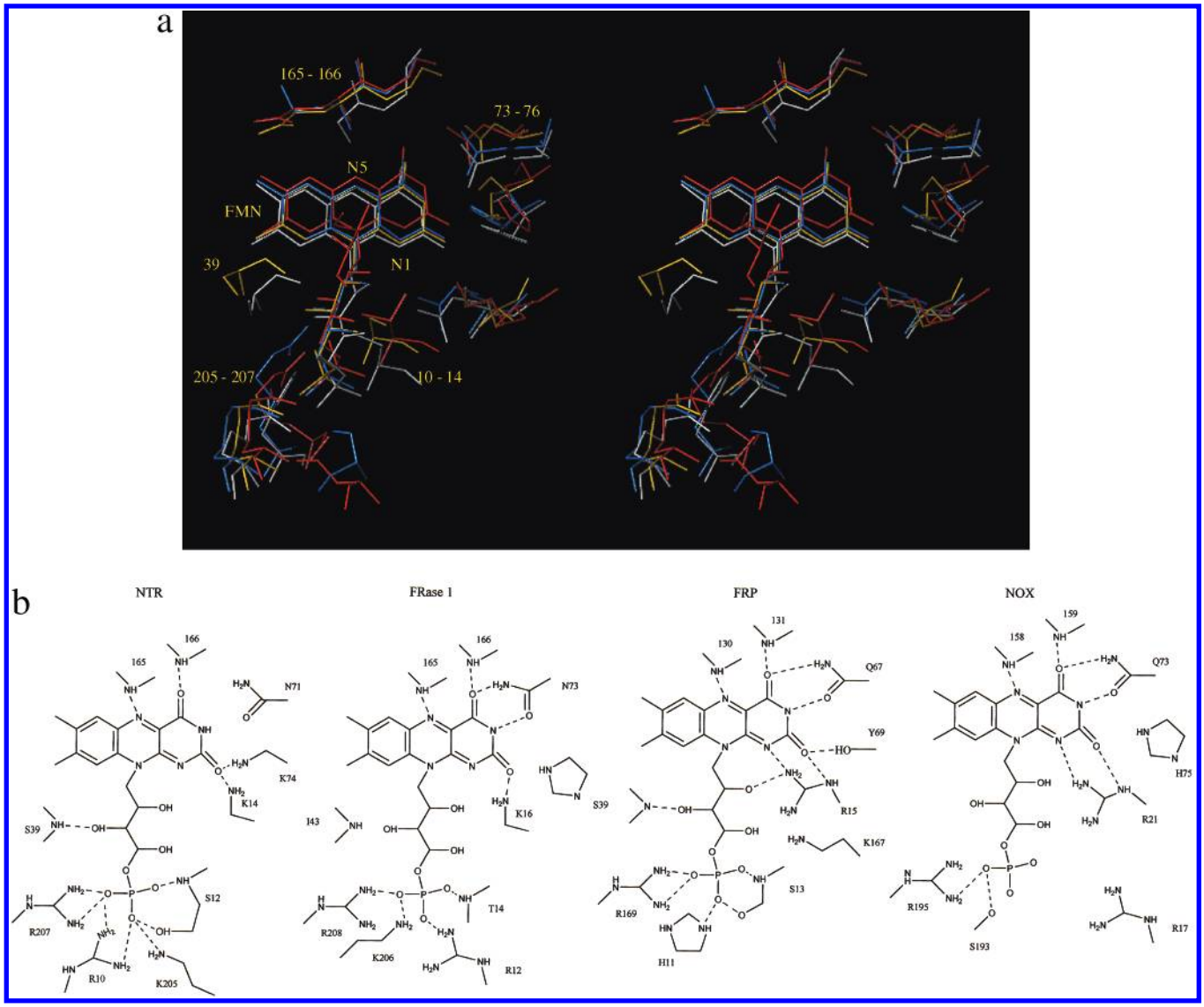

Figure 5. (a) Comparison of FMN binding pockets, overlaid on the FMN molecules, for the NTR, FRase 1, FRP, and NOX structures (gold, red, white, and blue, respectively). (b) Schematic diagram showing the interactions of FMN with amino acids in the active sites of the NTR, FRase 1, FRP, and NOX enzymes. Residues with potential hydrogen-bonding interactions < 3.3 Å to FMN are shown by dashed lines.

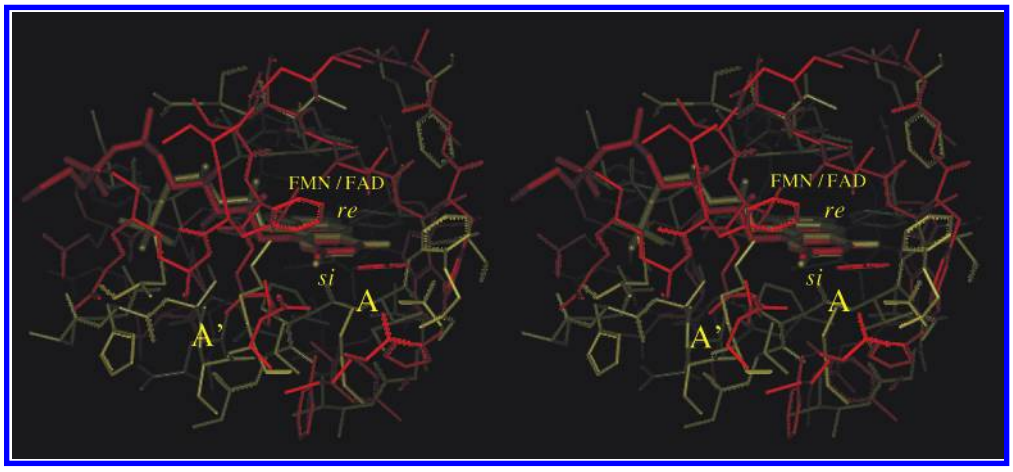

Figure 6. Comparison of the NTR and DT diaphorase[14] ligand binding pockets, based on the rms overlay between the flavin chromophore rings, colored gold and red, respectively. Openings providing access for ligands to the cofactor are labeled A for NTR and A′ for DT diaphorase. Only the *si* face of the flavin chromophore is accessible to potential ligands of DT diaphorase, while only the *re* face of the flavin chromophore is accessible in the structure.

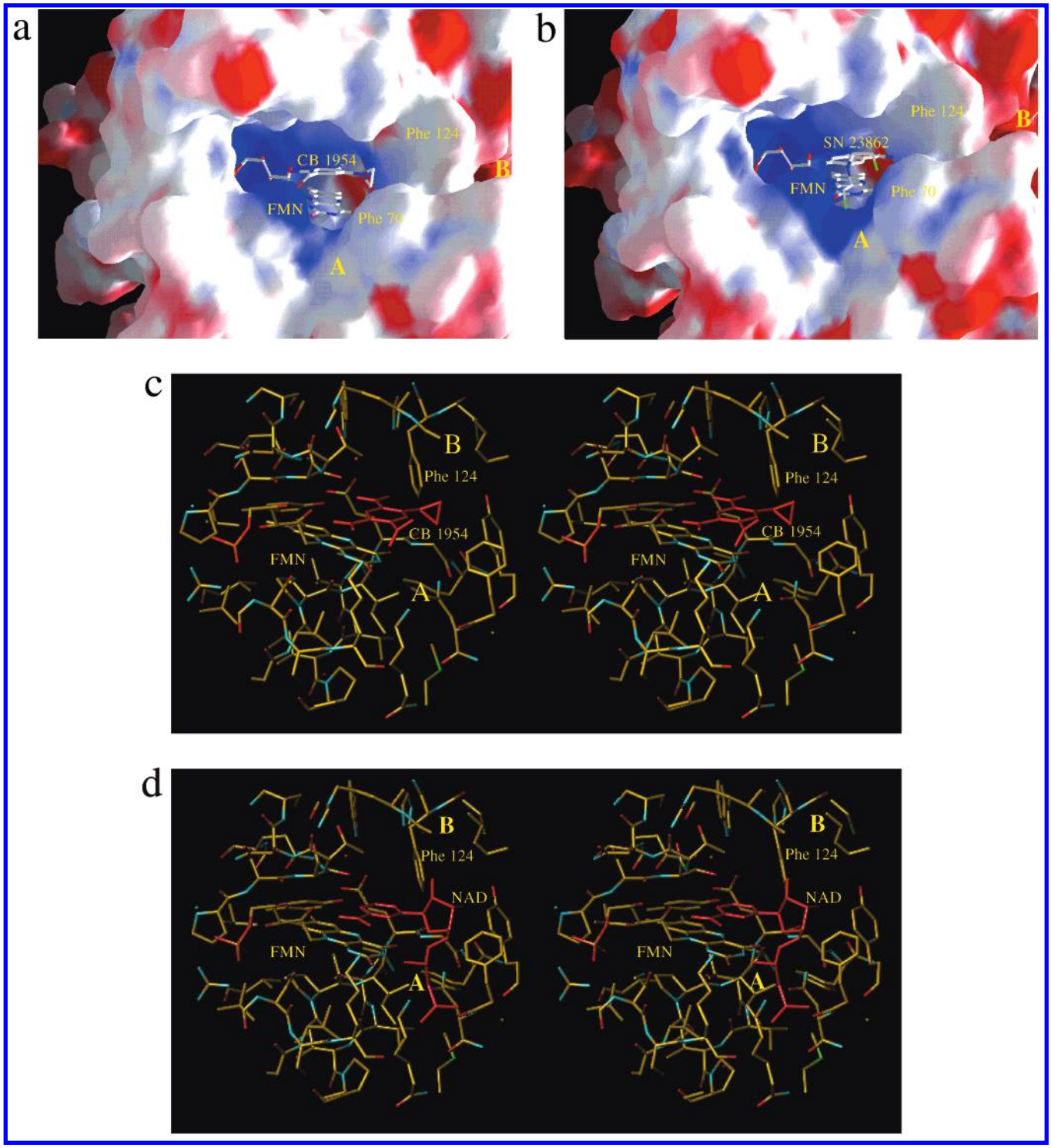

Figure 7. (a) Solvent-accessible surface representation of the substrate binding pocket, colored by charge and drawn with the GRASP program.[25] The regions of access to the FMN cofactor are labeled A and B. The prodrug CB1954 in shown modeled within the binding pocket, stacked over the FMN molecule, to highlight the potential access of the substrate to the FMN. (b) Solvent-accessible representaion of the substrate binding pocket, now showing the prodrug SN23862. (c) Stereodiagram showing the CB1954 molecule, colored red, modeled within the substrate binding pocket. (d) Substrate NAD, colored red, modeled within the binding pocket, in the absence of modifications to the protein side chain conformations.

kinetics for the prodrugs and inhibitors, using the information provided by the structural studies in combination with biochemical data.[4,11−13]

The compound dicoumarol has been frequently used in studies of NTR inhibition. It is a competitive inhibitor for prodrugs with the NTR enzyme and acts as a competitive inhibitor of all four enzymes in this family, suggesting a common method of inhibition, probably with the dicoumarol bound over the pyrimidine ring of FMN, as observed in the FRase 1 structure.[6] The enzyme DT diaphorase (NAD(P)H oxidoreductase) is a detoxifying enzyme which catalyzes the two-electron reduction of quinones. It is also competitively inhibited by dicoumarol, suggesting a common mode of inhibition for FMN-containing enzymes independent of the substrate binding pocket conformation.[14] We have compared

the features of the active sites of NTR and DT diaphorase. There are pronounced differences between the two. In the NTR family of structures the opening to the substrate-binding pocket points toward the O2, O4 carboxyl atoms of FMN, whereas access of substrates to FAD in the DT diaphorase structure is possible along the ribtyl chain, perpendicular to that of NTR. The most significant difference is that only the *re* face of the FMN molecule is accessible in the NTR structure, while only the *si* face of the FAD is accessible in the DT diaphorase structure. The two-electron reduction of similar ligands, with common modes of inhibition, can thus occur with both enzymes even though the conformation of the substrate binding pockets differs substantially (Figure 6). Dinitrobenzamides are being actively studied as prodrug candidates. These noncytotoxic prodrugs are activated by NTR with the reduction of their nitro groups to a hydroxylamine. They are then further activated by acetylation to form a cytotoxic DNA interstrand cross-linking agent. A number of studies have focused on the prodrug CB1954, an important candidate for GDEPT. It is activated by NTR to form either the 2- or 4-hydroxylamine. Once activated it cannot be further reduced. Activation of CB1954 by DT diaphorase in human cell lines is at a greatly reduced level: k_{cat} = 0.64 min^{-1} as compared to k_{cat} = 360 min^{-1} for *E. coli* NTR.[9,15] This explains both its ineffectiveness as a single agent drug in clinical trials and its utility in GDEPT approaches.

We have generated a molecular model of CB1954 and docked it into the active site of NTR. It is clear that the access channel is large enough to accommodate the prodrug (Figure 7a). There is also sufficient space to stack the prodrug over the pyrimidine ring of FMN with either N1 or N5 close to the nitro groups (Figure 7b,c). The reduction of the nitro group results in the formation of a hydroxylamine group limiting hydrogen bonding to O2′ of the FMN ribityl group.

The prodrug SN23862 (Figure 1, **2**) has a higher turnover[16] than CB1954, with a k_{cat} = 1580 min^{-1}, making it an improved GDEPT candidate. It is a difunctional alkylating agent, although only the 2-nitro group can be reduced by NTR to the 2-hydroxylamine. A molecular model of the prodrug SN23862 was placed into the substrate binding pocket to investigate the prodrug's higher k_{cat} and increased substrate specificity (Figure 7d). The attached mustard group on the prodrug sterically restricts the placement of the 4-nitro group over N5 of the FMN cofactor, while the 2-nitro group of the prodrug has unrestricted access. The addition of the mustard group does limit the number of orientations within the binding pocket that the prodrug can adopt and may explain an improved k_{cat}.

Both FRase 1 and NTR show the same enzyme kinetics for nitro- and quinone-containing compounds.[17] However the flavin kinetics were 30 times slower for NTR. Modification of Phe124 in NTR increases flavin reductase activity over 100-fold[18] to a level equivalent to that of FRase 1, while still retaining its nitroreductase activity (Figure 7a). This clearly shows the similarity of these two enzymes structurally and enzymatically. On the basis of sequence alignments, Phe124 in the homologous protein FRase 1 matches two consecutive Phe residues of the NTR protein. Residue Phe124 stacks over the aromatic ring of the inhibitor dicoumarol.[6] It is clear that single amino acid modifications within the FMN binding pocket can have broad effects on substrate specificity and kinetics.

Table 1. Crystallographic Data Set and Refinement Statistics[a]

space group	$P4_12_12$
unit cell parameters:	
a (Å)	57.74
b (Å)	57.74
c (Å)	275.51
data collection:	
max. resolution (Å)	1.85
no. of reflections	127222
no. of unique reflections	24109
completeness (%)	81 (50)
R_{merge} (%)	9.6
refinement:	
resolution range used (Å)	10−2.06
R_{all} (%)	20.3
R_{free} (%)	26.7
no. of atoms refined	3648
no. of waters	230
rms deviations from ideal geometry:	
bond distance rmsd (Å)	0.007
angle distance rmsd (deg)	1.21
dihedral rmsd (deg)	24.7
improper rmsd (deg)	1.16
$\langle B \rangle$, protein atoms (Å^2)	24
$\langle B \rangle$, solvent atoms (Å^2)	34

[a] Data set in parentheses refers to the highest resolution shell (2.3−2.16 Å): 1 $R_{all} = [\sum|F_o(hkl) - F_c(hkl)|]/\sum F_o(hkl)$; 2 $R_{merge} = [\sum I_i(hkl) - \langle I(hkl)\rangle]/\sum I_i(hkl)$.

Experimental Section

Crystallization and Data Collection. Protein expression, purification, crystallization, and space group determination of NTR from *E. coli.* has been previously outlined.[19] Crystallization of the enzyme was carried out at 4 °C by vapor diffusion in hanging drops equilibrated against 20% PEG 8000 in 50 mM potassium phosphate, pH 7.0. The space group is $P4_12_12$, or its enantiomorph $P4_32_12$, with unit cell dimensions of $a = b = 57.74$ Å and $c = 275.5$ Å. The asymmetric unit contains one homodimer, and V_m was calculated to be 2.39 Å^3 Da^{-1}. Crystals grew to approximately 0.4 mm × 0.4 mm × 0.2 mm. These were mounted in glass capillaries and data collected at 14 °C. The data set was collected on an R-AXIS II image plate with a double-focusing mirror system and an RU-200 rotating anode generator operating at 50 kV, 108 mA at the Molecular Structure Corp., Texas. Subsequent batches of purified enzyme provided two additional crystal forms. These were dependent upon the buffering pH. At pH 4.5 the space group is *P*1, with $a = 54.93$ Å, $b = 81.45$ Å, $c = 111.17$ Å, $\alpha = 74.9°$, $\beta = 76.9°$, and $\gamma = 70.8°$, with the asymmetric unit containing four homodimers. The third crystal form, grown at pH 7.0, is in the space group $P2_1$, with $a = 256.1$ Å, $b = 47.8$ Å, $c = 125.4$ Å, and $\beta = 108°$.

Structure Determination and Refinement. The crystal structure was solved by molecular replacement methods using the program X-PLOR,[20] employing the structure[6] of the NAD(P)H:FMN oxidoreductase of *Vibrio fischeri*[6] (Protein Data Bank entry code 1VFR). The search model selection was based on the 31.3% sequence identity between the two enzymes NTR and FRase 1 (Figure 2). PC refinement methods were used, where the search model consisted of the homodimer with a flexible linker between the two domains. Rotation searches were performed in space group *P*422 and provided an unambiguous solution. Translation searches were then performed in both $P4_12_12$ and its enantiomorph $P4_32_12$. An electron density map calculated from the top translation solution, in the space group $P4_12_12$, confirmed the model placement and space group. All subsequent refinement protocols were carried out using the programs X-PLOR version 3.1 and CNS. Rigid-body refinement using data to 3.0 Å resulted in an *R* factor of

48%. Before further refinement the model was rebuilt using the program TURBO.[21] Specific regions where differences such as insertions and deletions existed between the search model and NTR were omitted in the early rounds of positional and simulated refinement cycles. The cofactor FMN was also omitted at this initial stage. Refinement progressed smoothly with the gradual inclusion of the omitted regions, FMN, and finally water molecules. Data collection and refinement statistics are show in Table 1. Examination of the structure with PROCHECK version 2.0[22] showed no significant deviations from normality. A Ramachandran plot of the main torsion angles (φ, ψ) from PROCHECK revealed that 99.8% of non-glycine and proline residues are in the most favored or accepted regions. The atomic coordinates and observed structure factors for the nitroreductase have been deposited in the Protein Data Bank[23] with accession number 1DS7.

Acknowledgment. We thank Dr. Gillian Anlezark at the Centre for Applied Microbiology and Research (CAMR) for providing sufficient quantities of the purified protein to carry out this work. We also thank Dr. Richard Knox (Enzacta) for discussions at the outset of the project. The Cancer Research Campaign is thanked for support (Program Grant SP1384 to S.N.).

References

(1) Watanabe, M.; Ishidate, M.; Nohmi, T. A Sensitive Method for the Detection of Mutagenic Nitroarenes: Construction of Nitroreductase-overproducing Derivatives of Salmonella Typhimurium Strains TA98 and TA100. *Mutat. Res.* **1989**, *216*, 211−220.

(2) Bryant, C.; Hubbard, L.; McElroy, W. D. Cloning, Nucleotide Sequence, and Expression of the Nitroreductase Gene from Enterobacter Cloacae. *J. Biol. Chem.* **1991**, *266*, 4126−4130.

(3) Knox, R. J.; Friedlos, F.; Sherwood, R. F.; Melton, R. G.; Anlezark, G. M. The Bioactivation of 5-(Aziridin-1-yl)-2,4-dinitrobenzamide (CB1954) II. A Comparison of an Escherichia Coli Nitroreductase and Walker DT Diaphorase. *Biochem. Pharmacol.* **1992**, *44*, 2297−2301.

(4) Knox, R. J.; Friedlos, F.; Boland, M. P. The Bioactivation of CB 1954 and its Use as a Prodrug in Antibody-directed Enzyme Prodrug Therapy (ADEPT). *Cancer Metastasis Rev.* **1993**, *12*, 195−212.

(5) Altschul, S. F.; Gish, W.; Miller, W.; Myers, E. W.; Lipman, D. J. Basic Local Alignment Search Tool. *J. Mol. Biol.* **1990**, *215*, 403−410.

(6) Koike, H.; Sasaki, H.; Kobori, T.; Zenno, S.; Saigo, K.; Murphy, M. E. P.; Adman, E. T.; Tanokura, M. 1.8 Å Crystal Structure of the Major NAD(P)H:FMN Oxidoreductase of a Bioluminescent Bacterium, Vibrio Fischeri: Overall Structure, Cofactor and Substrate-analogue Binding, and Comparison with Related Flavoproteins. *J. Mol. Biol.* **1998**, *280*, 259−273.

(7) Hecht, H. J.; Erdmann, H.; Park H. J.; Sprinzl, M.; Schmid, R. D. Crystal Structure of NADH Oxidase from Thermus Thermophilus. *Nat. Struct. Biol.* **1995**, *2*, 1109−1114.

(8) Tanner, J. J.; Lei, B.; Shiao-Chun, T.; Krause, K. L. Flavin Reductase P: Structure of a Dimeric Enzyme that Reduces Flavin. *Biochemistry* **1996**, *35*, 13531−13539.

(9) Anlezark, G. M.; Melton, R. G.; Sherwood, R. F.; Coles, B.; Friedlos, F.; Knox, R. J. The Bioactivation of 5-(Aziridin-1-yl)-2,4-dinitrobenzamide (CB1954) I. Purification and Properties of a Nitroreductase Enzyme from Escherichia Coli − a Potential Enzyme for Antibody-directed Enzyme Prodrug Therapy (ADEPT). *Biochem. Pharmacol.* **1992**, *44*, 2289−2295.

(10) Simon, H.; Kraus, A. In *Isotopes in Organic Chemistry*; Buncel, E., Lee, C., Eds.; Elsevier Press: Amsterdam, 1976; Vol. 2, p 153.

(11) Peterson, F. J.; Mason, R. P.; Hovsepian, J.; Holtzman, J. L. Oxygen-sensitive and −Insensitive Nitroreduction by Escherichia Coli and Rat Hepatic Microsomes. *J. Biol. Chem.* **1979**, *254*, 4009−4014.

(12) Walsh, C. In *Enzymatic Reaction Mechanisms*; Bartlett, A. C., Ed.; W.H. Freeman & Co.: San Francisco, 1979; pp 362−405.

(13) Friedlos, F.; Denny, W. A.; Palmer, B. D.; Springer, C. J. Mustard Prodrugs for Activation by Escherichia Coli Nitroreductase in Gene-directed Enzyme Prodrug Therapy. *J. Med. Chem.* **1997**, *40*, 1270−1275.

(14) (a) Li, R.; Bianchet, M.; Talalay, P.; Amzel, L. M. The Three-dimensional Structure of NAD(P)H:quinone Reductase, a Flavoprotein Involved in Cancer Chemoprotection and Chemotherapy: Mechanism of the Two-electron Reduction. *Proc. Natl. Acad. Sci. U.S.A.* **1995**, *92*, 8846−8850. (b) Skelly, J. V.; Sanderson, M. R.; Suter, D. A.; Baumann, U.; Read, M. A.; Gregory, D. S. J.; Bennett, M.; Hobbs, S. M.; Neidle, S. Crystal Structure of Human DT-diaphorase: a Model for Interaction with the Cytotoxic Prodrug 5-(Aziridin-1-yl)-2,4-dinitrobenzamide (CB1954). *J. Med. Chem.* **1999**, *42*, 4325−4330.

(15) Boland, M. P.; Knox, R. J.; Roberts J. J. The Differences in Kinetics of Rat and Human DT Diaphorase Result in a Differential Sensitivity of Derived Cell Lines to CB 1954 (5-(Aziridin-1-yl)-2,4-dinitrobenzamide). *Biochem. Pharmacol.* **1991**, *41*, 867−875.

(16) Anlezark, G. M.; Melton, R. G.; Sherwood, R. F.; Wilson, W. R.; Denny, W. A.; Palmer, B. D.; Knox, R. J.; Friedlos, F.; Williams, A. Bioactivation of Dinitrobenzamide Mustards by an E. coli B Nitroreductase. *Biochem. Pharmacol.* **1995**, *50*, 609−618.

(17) Zenno, S.; Koike, H.; Tanokura, M.; Saigo, K. Gene Cloning, Purification, and Characterization of NfsB, a Minor Oxygen-insensitive Nitroreductase from Escherichia Coli, Similar in Biochemical Properties to FRase I, the Major Flavin Reductase in Vibrio Fischeri. *J. Biochem.* **1996**, *120*, 736−744.

(18) Zenno, S.; Koike, H.; Tanokura, M.; Saigo, K. Conversion of NfsB, a Minor Escherichia Coli Nitroreductase, to a Flavin Reductase Similar in Biochemical Properties to FRase I, the Major Flavin Reductase in Vibrio Fischeri, by a Single Amino Acid Substitution. *J. Bacteriol.* **1996**, *178*, 4731−4733.

(19) Skelly, J. V.; Collins, P. J.; Knox, R. J.; Anlezark, G. M.; Melton, R. G. Crystallization and Preliminary Crystallographic Data for an FMN-dependent Nitroreductase from Escherichia Coli B. *J. Mol. Biol.* **1994**, *238*, 852−853.

(20) Brünger, A. T. *X-PLOR, version 3.1. A System for X-ray Crystallography and NMR*; Yale University: Connecticut, 1992.

(21) Roussel, A.; Cambillau, C. TURBO−FRODO. In *Silicon Graphics Geometry Partners Directory*; Silicon Graphics: Mountain View, CA; pp 77−78.

(22) Laskowski, R. A.; MacArther, M. W.; Moss, D. S.; Thornton, J. M.. PROCHECK: a Program to Check the Stereochemical Quality of Protein Structures. *J. Appl. Crystallogr.* **1993**, *26*, 283−291.

(23) Berman, H. M.; Westbrook, J.; Feng, Z.; Gilliand, G.; Bhat, T. N.; Weissig, H.; Shindyalov, I. N.; Bourne, P. E. The Protein Data Bank. *Nucleic Acids Res.* **2000**, *28*, 235−242.

(24) Kraulis, P. J. MOLSCRIPT: a Program to Produce both Detailed and Schematic Plots of Protein Structures. *J. Appl. Crystallogr.* **1991**, *24*, 946−950.

(25) Nicholls, A.; Sharp, K. A.; Honig, B. Protein Folding and Association: Insights from the Interfacial and Thermodynamic Properties of Hydrocarbons. *Proteins* **1991**, *11*, 281−296.

JM000159M